THE JOURNAL OF PHYSICAL CHEMISTRY B

pubs.acs.org/JPCB Article

Charge Density of Cation Determines Inner versus Outer Shell Coordination to Phosphate in RNA

Published as part of The Journal of Physical Chemistry virtual special issue "Peter J. Rossky Festschrift".

Hung T. Nguyen and D. Thirumalai*

Cite This: *J. Phys. Chem. B* 2020, 124, 4114–4122 Read Online

ACCESS | Metrics & More | Article Recommendations

ABSTRACT: Divalent cations are often required to fold RNA, which is a highly charged polyanion. Condensation of ions, such as Mg^{2+} or Ca^{2+}, in the vicinity of RNA renormalizes the effective charges on the phosphate groups, thus minimizing the intra RNA electrostatic repulsion. The prevailing view is that divalent ions bind diffusively in a nonspecific manner. In sharp contrast, we arrive at the exact opposite conclusion using a theory for the interaction of ions with the phosphate groups using RISM theory in conjunction with simulations based on an accurate three-interaction-site RNA model. The divalent ions bind in a nucleotide-specific manner using either the inner (partially dehydrated) or outer (fully hydrated) shell coordination. The high charge density Mg^{2+} ion has a preference to bind to the outer shell, whereas the opposite is the case for Ca^{2+}. Surprisingly, we find that bridging interactions, involving ions that are coordinated to two or more phosphate groups, play a crucial role in maintaining the integrity of the folded state. Their importance could become increasingly prominent as the size of the RNA increases. Because the modes of interaction of divalent ions with DNA are likely to be similar, we propose that specific inner and outer shell coordination could play a role in DNA condensation, and perhaps genome organization as well.

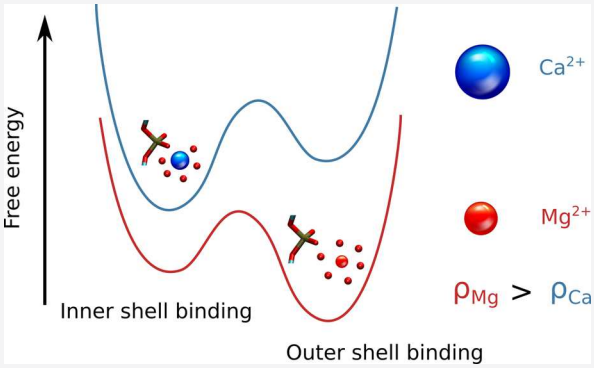

INTRODUCTION

How RNA molecules, containing only four bases with similar chemical properties, fold into a bewildering variety of complex structures continues to be a fascinating and unsolved problem.[1,2] Because RNA molecules are polyanions, they require counterions to fold. In particular, divalent cations are required to mute the repulsive electrostatic interactions between the negatively charged phosphate groups so that RNA can reach the folded state. As a consequence, ion−RNA interactions during the folding process have been the subject of extensive experimental and theoretical studies.[3−21]

From the theory of ion-induced shape changes in polyelectrolytes (PEs), it follows that divalent ions (such as Mg^{2+} and Ca^{2+}) should be more efficient than monovalent ions in neutralizing the phosphate charges in RNAs.[22,23] The physically appealing counterion condensation (CIC) theory could be used to estimate the fraction of condensed ions onto PEs with regular (rod-like or spherical) shape and account for the phenomenon of entropically driven counterion release in which monovalent ions are replaced by divalent ions. However, the CIC theory cannot be used in problems involving dramatic shape changes (RNA folding or PE collapse) as the ion concentration is altered. More importantly, the CIC assumes that the counterions uniformly decorate the polyanion, which is certainly valid for rod-like PEs. Because of the clear physics of the CIC theory, the prevalent view in the RNA literature is that most of the ions are uniformly (sometimes referred to as diffusive ions) condensed onto RNA. Although the CIC theory does estimate the extent of charge renormalization of the phosphate groups,[4,24] it gives a qualitatively incorrect picture of the mechanism by which divalent cations drive RNA folding.[2,25]

Recently, simulations of a large ribozyme and several other RNA constructs, in the presence of both monovalent and divalent ions, have shown that the ions have a strong propensity to bind to nucleotides in a site-specific manner, and not uniformly.[25−27] The irregular shape of the RNA plays an important role in determining where the ions bind, as the

Received: March 17, 2020
Revised: April 25, 2020
Published: April 28, 2020

https://dx.doi.org/10.1021/acs.jpcb.0c02371
J. Phys. Chem. B 2020, 124, 4114–4122

ions are naturally drawn to the highly negatively charged pockets. Other studies, focusing only on the folded states or well-defined complexes involving RNA, have shown that the site-specifically bound Mg^{2+} ions to various RNA molecules are stable.[28−33] In particular, two recent studies show that there ought to be Mg^{2+} ions in the active sites of the pistol and Varkud Satellite ribozymes, even though they were not detected in crystal structures.[34,35] Subsequent experiments validated this prediction providing a mechanistic basis for the requirement of Mg^{2+} in catalysis. However, these studies did not consider ion-driven folding of RNA from a completely unfolded state, which is the subject of our interest here and elsewhere.[25,26] In order to develop a quantitative theory of RNA folding, effects of ions and the associated conformational changes they induce in RNA must be treated on equal footing.

Conceptually, specific association of divalent ions to RNAs could be categorized into two binding types: inner shell (or inner sphere) binding where the divalent ion is partially dehydrated to interact directly with one (or more) atom of the RNA and outer shell (or outer sphere) where it fully retains its first hydration shell to bind the RNA (illustrated in Figure 1A).[9] Inner shell binding of Mg^{2+} has been mostly detected in relatively large RNAs, where the ions are often localized at the deepest regions inside the RNAs.[36] Characterizing which binding types the ions utilize to bind RNAs is difficult and requires reliable computational methods because currently experimental techniques cannot easily distinguish between the two coordination modes.

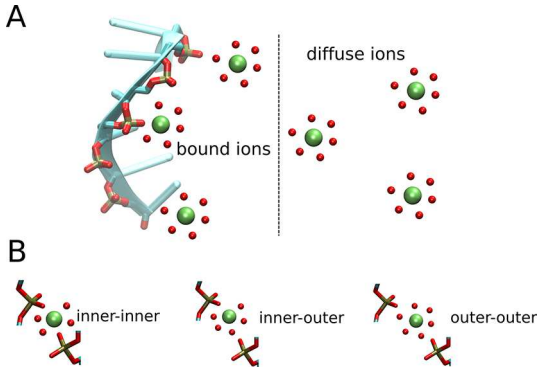

Figure 1. Schematic classification of divalent cations that interact with RNA. (A) Bound ions bind directly to the RNA in either the inner shell or outer shell binding. Diffuse ions, with intact hydration shells, are located further away from the RNA surface, interacting mainly with the RNA electrostatic field. For clarity, only water molecules in the first hydration shell of the ions are shown. (B) In some cases, a single ion could bind two phosphate groups simultaneously, resulting in bridging interaction. We refer to these ions as bridging ions.

Divalent-ion-driven folding of RNA is a strongly interacting many body problem because the binding of several Mg^{2+} ions in a specific and correlated manner is needed to obtain a stable folded structure.[25,26] Already at the single ion level, the interplay between the inner and outer sphere coordination manifests itself. In a pioneering series of studies conducted nearly 30 years ago, Rossky and co-workers used extended reference interaction site model (RISM) theory and simulations to show that the potential of mean force (PMF) between Na^+ and phosphate exhibits the two binding modes mentioned above.[37−39] Building on these studies, we have recently developed a theory accounting for both types of binding between divalent ions and phosphate groups in RNAs.[40] The theory, when incorporated in a thermodynamically accurate three interaction site (TIS) force field for RNA,[41] quantitatively reproduced ion-dependent RNA folding thermodynamics for several RNA molecules with different sizes, ranging from a small pseudoknot to the aptamer domain of the adenine riboswitch. We showed that both the inner and outer shell bindings are needed to produce a faithful description of ion−RNA interactions, because the ion−RNA interaction free energies and therefore the RNA folding process depend sensitively on the ion−phosphate potential.

In this study, we focus on the mechanism of divalent cation condensation around RNA in order to investigate the ion binding modes to the phosphate groups (inner or outer shell). We show that the divalent ion charge density as well as the RNA size determine the extent of inner versus outer shell binding to the phosphate groups. For small RNAs, such as the Beet Western Yellow Virus (BWYV) pseudoknot (PK), Mg^{2+} ions show a stronger propensity to bind to the outer shell. For larger RNAs, such as the 58-nucleotide fragment of the rRNA (58-nt rRNA), there is a shift in favor of the inner shell binding, because of an increased number of nearby phosphate groups in a larger RNA presumably compensating for the high penalty of ion dehydration. In contrast, Ca^{2+} ion, which has a larger radius and smaller charge density compared to Mg^{2+}, dehydrates more readily to bind directly to the phosphate groups in the inner shell regardless of the RNA size. We also find that the bridging divalent ions, which bind two (or more) non-neighboring phosphate groups simultaneously, play a crucial role in stabilizing the RNA tertiary structure. Diluting the divalent ion concentration leads to a smaller probability of finding these bridging ions, thus destabilizing the folded state.

COMPUTATIONAL DETAILS

Divalent Ion−Phosphate Interaction. Accurate simulations using coarse-grained models of ribozymes in explicit monovalent and divalent cations are computationally demanding.[25,26] In order to simplify the problem, while still retaining a high level of accuracy in predicting the RNA folding thermodynamics and kinetics, we developed a theory to treat the electrostatic interactions involving monovalent ions implicitly, while treating the many body effects due to divalent ions explicitly.[40] Briefly, we assumed that the screening effect due to monovalent cations, especially when present at high concentrations, can be described by the classical Debye−Hückel (DH) theory. However, an accurate theory is required to treat the short-ranged divalent ion−phosphate interaction, where the ion−ion correlation and charge polarization are important. We used RISM[37−39,42,43] to calculate the short-ranged interaction between the divalent ion and the phosphate group and smoothly join it to the DH potential at large separations. The resulting PMF between the cation X^{2+} and the phosphate group is given by[40]

$$V_{X-P}(r) = W(r) + [U_{DH}(r) - W(r)] \exp\left(-\frac{a^2}{r^2}\right) \quad (1)$$

where $W(r)$ is the PMF calculated using the RISM theory and $U_{DH}(r)$ is the DH potential between X^{2+}−P accounting for the screening effect of monovalent ions. Our earlier work showed that the use of eq 1 in conjunction with the TIS model for RNA quantitatively reproduced the folding thermodynamics of several RNA molecules over a wide range of monovalent and

https://dx.doi.org/10.1021/acs.jpcb.0c02371
J. Phys. Chem. B 2020, 124, 4114−4122

divalent ion concentrations.[40] Separation of long-range potentials into a short-ranged part and the smoother long-ranged part had been previously proposed in several insightful studies.[44,45] More recently, Gao et al. have applied the local molecular field treatment to calculate the PMF between Ca^{2+} and Cl^-.[46] The interesting finding is that a judiciously chosen short-range potential in a system dominated by electrostatic interactions suffices to capture the physics of cation−anion interactions. Our work, which is similar in spirit, uses RISM to calculate the PMF between Mg^{2+}/Ca^{2+} and phosphates in the monovalent salt buffer, which is needed to investigate RNA folding.

RNA Force Field and Simulation Details. *Model.* Since the details of the force field and simulations are given elsewhere,[40] we only provide a brief description here. We used the TIS model in which each nucleotide is coarse-grained by three beads corresponding to phosphate, sugar, and base moieties.[41] The energy function in the TIS model is $U = U_{BA} + U_{EV} + U_{ST} + U_{HB} + U_{EL}$, where U_{BA} takes into account the bond and angle restraints between connected beads and U_{EV} is the excluded volume term. Stacking and hydrogen bond interactions, U_{ST} and U_{HB}, were calibrated to reproduce the heat capacity curves of small RNAs.[47] Once the two parameters were determined, we kept them unchanged for all RNA constructs. Thus, the model is transferable and could be used to study the folding of much larger RNA molecules.[25,26] The electrostatic term U_{EL} is the sum of the DH energies for all of the charges excluding the divalent ion−P term, which is calculated using eq 1.

Simulations. We performed simulations by integrating the Langevin equations of motion. Divalent cations were initially added randomly to a cubic box containing a RNA molecule of interest. The initial coordinates of the RNA were taken from the structure of the folded state in the PDB, 1L2X and 1HC8 for the 28-nt BWYV PK and 58-nt rRNA, respectively. The box size varied from 700 to 3000 Å, depending on the bulk concentration of divalent cations. We used large enough boxes to ensure that at least 200 divalent cations were present in the simulations. We used periodic boundary conditions to minimize the effect of finite box size. Numerical integration of the equations of motion was performed using the leapfrog algorithm. We carried out low-friction dynamics in order to increase the sampling efficiency of the conformations, in which the viscosity of water was reduced 100 times.[48] Snapshots were taken every 10,000 steps, and the last two-thirds were used to calculate various quantities of interest.

Analyses. The local concentration of divalent ions around the ith nucleotide in the RNA was computed using

$$c_i = g_{X-P,i}(r_0)C_2 \quad (2)$$

where C_2 is the bulk concentration of divalent ions and $g_{X-P,i}(r)$ is the radial distribution function of X^{2+} around the ith phosphate group. The value r_0 corresponds to the first or second peak in $g_{X-P,i}(r)$, depending on the binding mode.

RESULTS

Divalent Cation Distribution around RNA Is Site-Specific. Figure 2A shows the concentration profiles of Mg^{2+} from the center of BWYV PK. Although the bulk concentration is low (on the order of sub-mM), the local concentration of Mg^{2+} ions is ∼3 orders of magnitude larger, indicating that the ions are strongly attracted to the PK. Interestingly, parts B and C of Figure 2 illustrate that the distribution of Mg^{2+} ions around BWYV is not uniform but site-specific. The fingerprints in Figure 2B exhibit peaks at nucleotide positions G7, G12, and C22 for the folded state. These nucleotides are located at the central positions in the RNA structure (shown in Figure 2C), where there are several phosphate groups surrounding them, thus resulting in strong negative electrostatic potential. These three residues glue the two stems and loops together, maintaining the structural stability of the PK. Had the ion condensation been uniform, then the peaks in Figure 2B would be absent, and the distribution would be uniform, which clearly is not the case.

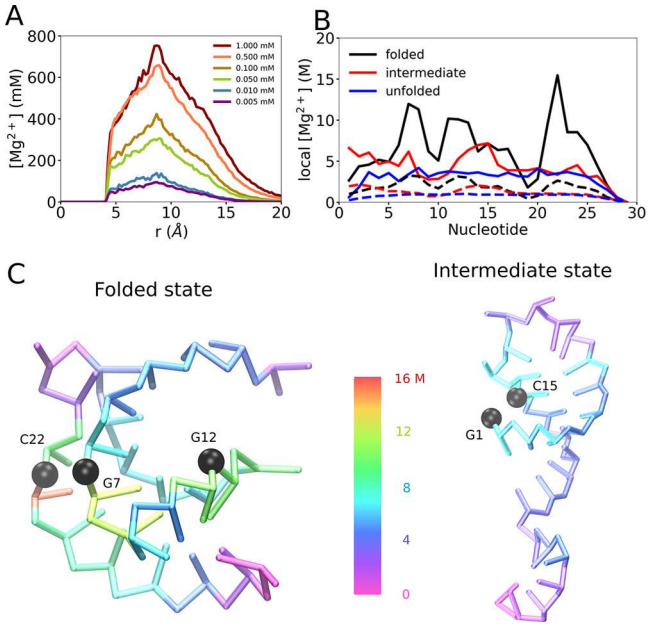

Figure 2. (A) Concentration profiles of Mg^{2+} relative to the geometric center of the BWYV pseudoknot at various bulk concentrations. The local concentration of Mg^{2+} is around 3 orders of magnitude larger than the bulk concentration, implying that the ions are strongly attracted to the PK. (B) Local concentration (eq 2) of Mg^{2+} in the inner shell (solid lines) and outer shell (dashed lines) computed for each nucleotide position at 54 mM KCl and 1.0 mM Mg^{2+}. (C) Map of inner shell concentrations (M) onto representative snapshots of the folded and intermediate states at $[Mg^{2+}]$ = 1.0 mM. Phosphate groups of a few key nucleotides are shown in black spheres. The results indicate that binding of Mg^{2+} to RNA is highly nucleotide-specific, in contrast to the CIC theory.

The Mg^{2+} concentration profiles for the intermediate and unfolded states are different compared to the folded state despite having the same bulk concentration. Because of the extended conformations, the unfolded state does not show any interesting feature in the profiles, and the Mg^{2+} ions have almost uniform binding affinities to all of the nucleotides except near the 5′ and 3′ regions where the chain-end effects might be important. The profile of the intermediate state, adopting mostly hairpin conformations (shown in Figure 2C), shows peaks at nucleotides G1 and C15, because of the formation of the hairpin leading to a high accumulation of phosphate groups around these nucleotides. The presence of ion peaks in the intermediate states shows that, as soon as the titration starts, Mg^{2+} binds to specific nucleotides with high probability. When the RNA folds from the intermediate state to the folded state, there is an interesting shift in the fingerprint of Mg^{2+}.

https://dx.doi.org/10.1021/acs.jpcb.0c02371
J. Phys. Chem. B 2020, 124, 4114−4122

Similar binding patterns are also observed for the case of 58-nt rRNA (Figure 3). In this case, because the RNA folding depends on Mg^{2+} ions,[40,49] new Mg^{2+} binding sites emerge as the ion concentration increases, leading to significant RNA compaction. Since the conformational changes occur when the Mg^{2+} (or monovalent ion) concentration varies, one might expect there should be a binding pattern shift if the Mg^{2+} concentration changes. Indeed, this is the case. Figure 3A shows the local concentration of Mg^{2+} ions in the inner shell at two different bulk concentrations, 1.0 mM where the rRNA is fully folded and 0.02 mM where the rRNA mostly samples secondary structures. There are some notable differences in the two concentration profiles, especially at nucleotide positions that play key roles in maintaining the RNA tertiary structure. In the folded structure, G121 is located right at the intersection between the two stems and plays an extremely important role bridging the tertiary structure together, forming a Hoogsteen basepair with G141 and stacking on top of A139. (G137 glues the other two stems but is located outside this region.) The phosphate groups of U147 and A148 point directly toward this region, where there is an overwhelming presence of other phosphate groups. This suggests that this region has a strong negative electrostatic potential, thus requiring excessive counterions to neutralize and stabilize the overall structure (Figure 3B). We note that it is this region that gives rise to the difference in Mg^{2+} fingerprints when the Mg^{2+} concentration varies.

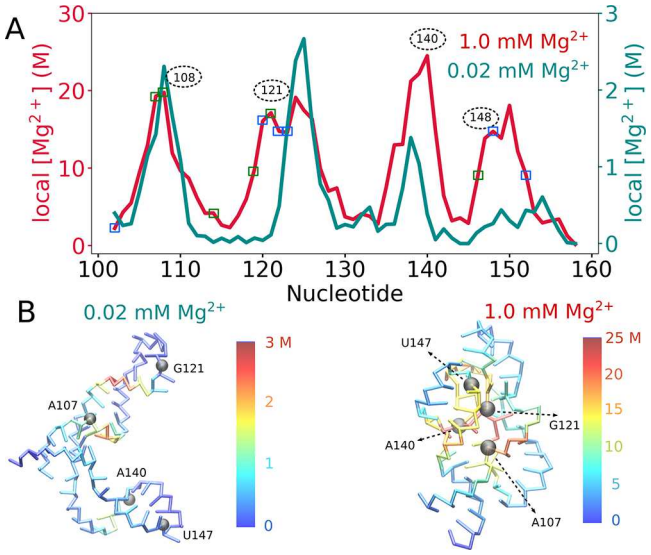

Figure 3. Fingerprint of Mg^{2+} binding to 58-nt rRNA. (A) Mg^{2+} local concentration in the inner shell at two concentrations, 1.0 mM (red, left axis) and 0.02 mM (blue, right axis). Note that the scales associated with the two axes are different. Small blue and green squares correspond to positions in the crystal structure where Mg^{2+} ions bind using inner and outer spheres, respectively. At 1.0 mM Mg^{2+} concentration, the rRNA remains folded, whereas it partially unfolds at 0.02 mM Mg^{2+}. Surprisingly, the ion binding patterns are similar except at some key nucleotides: A107, G121, A140, and U147, which are located at important positions in the rRNA structure. The phosphate groups in these nucleotides are highlighted as gray spheres in part B. Reducing the bulk Mg^{2+} concentration leads to the RNA unfolding, therefore altering the ion binding pattern. This is clearly illustrated in part B, which shows the local concentration of Mg^{2+} ions mapped onto representative structures of the rRNA at 0.02 mM (left) and 1.0 mM (right) Mg^{2+} bulk concentration. Each residue is colored based on the local concentration of Mg^{2+} bound to its phosphate group.

Inner Shell vs Outer Shell Binding Depends on the Charge Density of Divalent Ions. Do divalent ions interact with RNA directly or in the hydrated form? It is widely known that, in aqueous solution, Mg^{2+} ion exists mainly in the hexahydrated form, $Mg(H_2O)_6^{2+}$, because it has a large favorable hydration free energy. Due to the high density charge, it would need a highly negatively charged environment (such as in large RNAs) in order to even partially dehydrate the Mg^{2+} ion. The lifetime of water coordinated to other divalent cations, which have a larger radius and therefore a smaller charge density, is relatively short.[50] Consequently, such ions (Ca^{2+}, for example) readily dehydrate and could bind directly to the phosphate groups through inner shell coordination. Currently, most (if not all) knowledge about the inner shell binding of divalent cations comes mainly from X-ray crystallography, where the divalent ion location is assigned from the electron density map. Such an assignment for Mg^{2+} needs extra care to distinguish Mg^{2+} ion from isoelectronic species (having the same number of electrons) such as Na^+, NH_4^+, and water, which are usually present in an excess amount compared to Mg^{2+} in solution.[51,52] Since our model describes both the inner and outer shells of Mg^{2+} around phosphate groups, we can determine how and where Mg^{2+} ions are localized around the phosphate groups in RNA.

Figure 4A shows the radial distribution function between divalent ions and the P groups in BWYV PK. We performed the calculations for Mg^{2+} and Ca^{2+}, although any spherical ion could be treated using our theory. It is obvious that our model accounts for both the inner and outer shell binding. We stress that it is crucial to treat both of the binding modes on equal footing in order to reproduce ion−RNA binding thermodynamics.[40]

We computed the total number of ions in each binding mode for BWYV PK. If the ion−P distance falls within the first peak in $g_{X-P}(r)$ ($r < 3.2$ Å for Mg^{2+}, $r < 3.7$ Å for Ca^{2+}), then the ion is considered to be in the inner shell. If it is within the second peak (3.2 Å $\leq r <$ 6.0 Å for Mg^{2+}, 3.7 Å $\leq r <$ 6.6 Å for Ca^{2+}), then the ion binds in the outer shell. Interestingly, some ions bind to the inner shell of one phosphate and to the outer shell of another phosphate group. We consider such ions as belonging to the inner shell. Figure 4B shows that Mg^{2+} has a tendency to bind using the outer shell, even though we also find some ions that bind directly to the phosphates in the inner coordination. In contrast, Ca^{2+} prefers binding directly to phosphate groups without water mediation. The higher charge density of Mg^{2+} ion, compared to Ca^{2+} ion, results in stronger interaction with water than Ca^{2+}, thus shifting the binding pattern toward the outer shell interaction. The result is in agreement with the crystal structure of BWYV where there are a total of six Mg^{2+} ions and three of them bind directly to the phosphate groups, while the remaining three bind in the hexahydrated form.[53] It should be noted, however, that the conditions used in obtaining the crystal structure are different from those in the solution, and additional experimental data may be needed to confirm our predictions.

Figure 4C shows the number of divalent ions found in the inner (N_{in}) or outer shell (N_{out}) at different bulk concentrations. We also calculated the number of diffuse ions, which are located at least two hydration shells away from the RNA surface, using $N_{X,diff} = \Gamma_X - N_{X,in} - N_{X,out}$, where Γ_X is the preferential interaction coefficient for divalent ion X^{2+},

https://dx.doi.org/10.1021/acs.jpcb.0c02371
J. Phys. Chem. B 2020, 124, 4114−4122

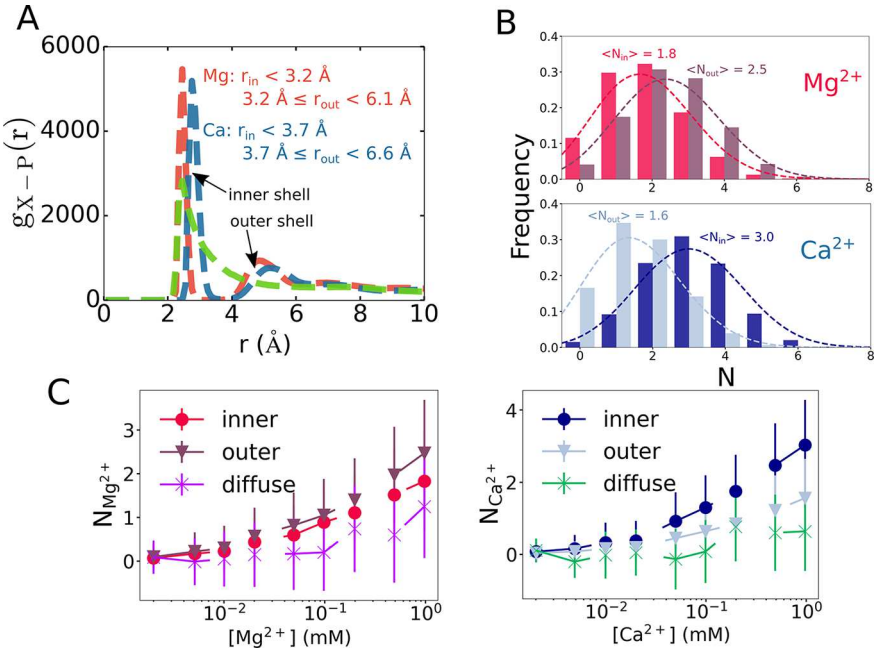

Figure 4. (A) Radial distribution function $g_{X-P}(r)$ of divalent ions around phosphate groups in the BWYV pseudoknot. Calculations were performed for 1.0 mM Mg^{2+} or Ca^{2+} in 54 mM KCl. For completeness, we also show $g(r)$ for Mg^{2+} using the Debye−Hückel potential (green dashed curve). There are two peaks corresponding to the inner and outer sphere coordination of Mg^{2+} to phosphate groups. (B) Histogram of Mg^{2+} and Ca^{2+} ions in the inner, N_{in}, and outer shell, N_{out}. An ion is defined to be in the inner or outer shell if the ion−phosphate distance falls within the first or second peak of $g_{X-P}(r)$, respectively, as indicated in part A. (C) Averaged values of N_{in} and N_{out} at different bulk concentrations for Mg^{2+} and Ca^{2+}. We also show the number of diffuse ions, which are located at least two hydration shells away from the RNA surface. Our simulations predict that the majority of divalent cations binds to RNA using either the inner or outer sphere coordination, in sharp contrast to the CIC theory.

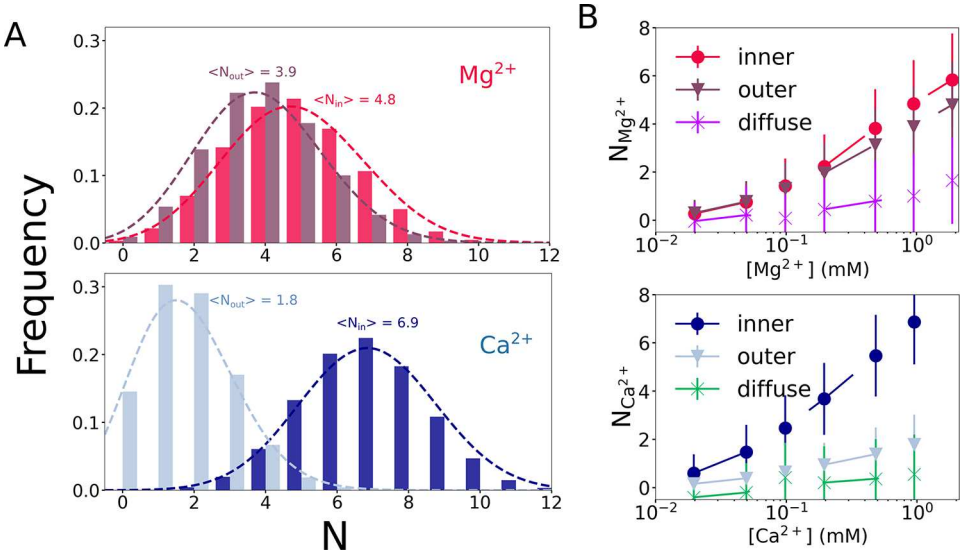

Figure 5. (A) Histograms of Mg^{2+} and Ca^{2+} coordination to the inner and outer shell at 1.0 mM divalent ions concentration for the 58-nt rRNA. Just as in the case for BWYV, Mg^{2+} binds to the rRNA using both inner and outer shell coordinations, whereas Ca^{2+} strongly favors the inner shell binding. (B) Averaged values of N_{in}, N_{out}, and the number of diffuse ions at different bulk concentrations for Mg^{2+} and Ca^{2+}. Remarkably, the average number of diffuse ions is negligible, which further underscores the importance of specific binding.

which is equivalent to the excess number of divalent ions attracted to the RNA, regardless of the position of the ions (data available elsewhere[40]). It can be seen from the results in Figure 4C that the number of diffuse ions is low even at high bulk concentrations for both ions, suggesting that divalent ions bind to RNA directly either via inner or outer shell binding. This agrees with our recent findings that, in general, divalent cations are strongly attracted and bind RNAs directly and specifically, while the major role of monovalent ions is to screen the electrostatic propulsion between the phosphate groups.[25] It also supports the picture from X-ray scattering measurements that divalent cations are generally localized closer to the RNA/DNA than monovalent ions.[54,55]

An interesting result is revealed when we investigate ion binding to the 58-nt rRNA (shown in Figure 5), which is larger than BWYV. Figure 5A shows that, for this RNA, Mg^{2+}

https://dx.doi.org/10.1021/acs.jpcb.0c02371
J. Phys. Chem. B 2020, 124, 4114−4122

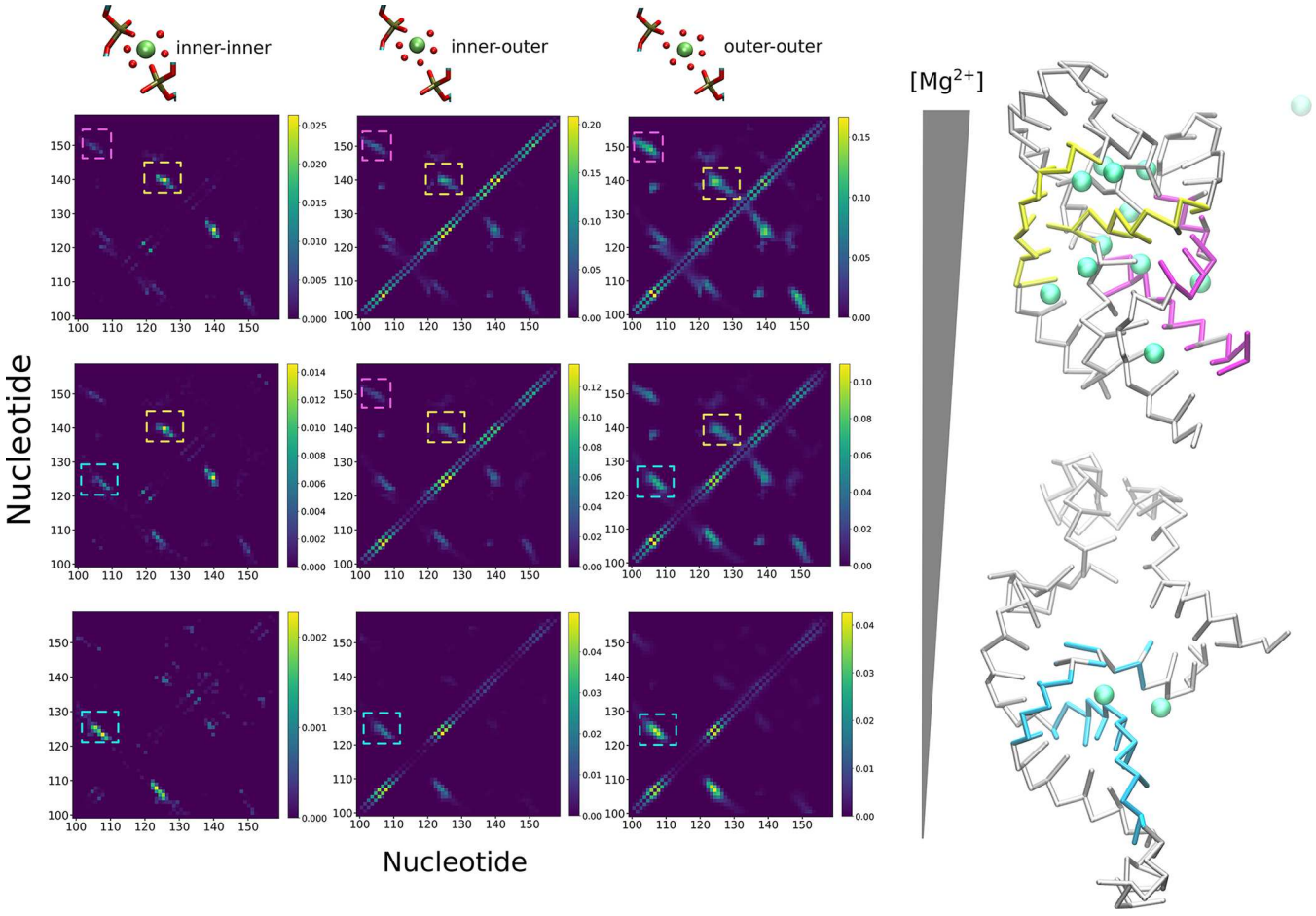

Figure 6. Role of bridging Mg^{2+} ions on 58-nt rRNA folding. Shown here is the heat map of where the bridging ions are found. The color bars on the right of each panel denote the bridging probability. On the left is the inner−inner bridging ion, where Mg^{2+} binds two phosphate groups in the inner shell simultaneously. Inner−outer bridging is shown in the middle, where Mg^{2+} binds one phosphate group in the inner shell and another using the outer shell coordination. In the outer−outer bridging (right), Mg^{2+} ions are coordinated to both groups using the outer shell. From top to bottom, the bulk concentration of Mg^{2+} decreases from 1.0 mM to 0.10 mM to 0.010 mM in a buffer containing 60 mM KCl. The color intensity is varied for different bulk concentrations, so the lower concentrations appear to have the same color intensity, but the actual probability is lower (see the color bars). Such a representation highlights the change in the bridging pattern as the RNA unfolds. The two most likely conformations on the right are in high and low Mg^{2+} concentrations, respectively. The Mg^{2+} ions are depicted as green spheres. Parts of the structures that are colored purple, yellow, and blue are regions that form bridging interactions and are denoted by colored dashed squares in the heat map. There are three bridging Mg^{2+} ions in the crystal structure, which are located precisely in the purple and yellow regions.

partially dehydrates and binds to the phosphates more readily using the inner coordination than the outer shell binding. The difference could be explained by the following arguments. BWYV is a relatively small 28-nucleotide RNA with a simple open structure (Figure 2C). The majority of the Mg^{2+} ions, consequently, stays near the RNA surface because there is no deep pocket with high electrostatic potential. As a result, only a couple of ions, which are located near the RNA center, dehydrate and bind using the inner shell. On the other hand, the rRNA is more complex, with a structure that has more deep pockets with highly negative electrostatic potential surrounded by a large number of phosphate groups (Figure 3B). These regions need to be stabilized by small sized ions with a large charge density in order for the RNA to stabilize the folded state. The high penalty associated with Mg^{2+} dehydration is partly (or even fully) compensated if the ion is attracted toward these regions. This could also partly explain why the 58-nt rRNA requires Mg^{2+} to fold. On the other hand, the majority of Ca^{2+} ions predominantly interacts directly with phosphate groups using the inner shell coordination. Compared with BWYV, the binding preference of both ions features a slight shift toward the inner shell, which is expected for larger RNA molecules that require divalent ions to maintain their structural integrity.

Bridging Divalent Cations Contribute to RNA Stability. Ions that interact with RNAs are usually classified as diffuse and bound ions (Figure 1). The bound ions can be further divided into outer shell and inner shell binding. Bridging interactions come from a bound ion that simultaneously interacts with two (or more) phosphate groups. Both phosphate groups could bind the ion in the inner shell or the outer shell, which we call inner−inner or outer−outer bridging, respectively. In addition, the ion could also bind one phosphate in the inner shell while coordinating with another using the outer shell. We refer to this mode of bridging as inner−outer shell bridging. As we showed in previous sections, the divalent cations interact with RNAs via exclusively specific and direct bindings, either by inner shell or outer shell coordination. Consequently, we expect that the probability of divalent ions staying in the bridging position is high. Because

https://dx.doi.org/10.1021/acs.jpcb.0c02371
J. Phys. Chem. B 2020, 124, 4114−4122

the folding of the 58-nt RNA (and presumably other larger RNAs) depends strongly on Mg^{2+} ions, we propose that the bridging ions would be crucial in bridging distant nucleotides in order to form stable tertiary structures.

We calculated the probability of finding the bridging ions for any two nucleotides in the rRNA. Figure 6 plots the results for inner−inner, inner−outer, and outer−outer bridging as a function of Mg^{2+} concentration. At high Mg^{2+} concentration (1.0 and 0.1 mM), the rRNA remains mostly in the folded state, whereas, at low Mg^{2+} concentration (0.01 mM), it partially unfolds and populates extended states. The heat map at high concentrations reveals two regions where the bridging Mg^{2+} ions stabilize the folded state (yellow and purple squares in Figure 6). Remarkably, we also found three bridging Mg^{2+} ions located exactly at these regions in the crystal structure. Two of them are the inner−outer bridging ions, which connect A123−A146 and A148−G121. The last one is an outer−outer bridging ion, gluing A107 and G149. Other interesting points can be made from the results in Figure 6. First, as the ion concentration decreases, the probability of finding the bridging ions goes down as well. (We note that the color intensity for different ion concentrations is different; therefore, we refer to the color bars for the actual values of the probabilities. We intentionally chose the color scales to demonstrate the clear shift in the bridging pattern under low ion concentration conditions.) This holds for all inner−inner, inner−outer, and outer−outer bridging. The obvious reason is that, as the ion concentration is lowered, the equilibrium is shifted to the unfolded states. Therefore, the attraction between the RNA and Mg^{2+} ions is weakened, leading to a smaller number of condensed ions. Second, it is rare to find a Mg^{2+} ion dehydrating two water molecules in the hydration shell simultaneously in order to bind two phosphate groups in the inner shell. The largest probability we observed in the simulations for such an event is ∼2% at the highest Mg^{2+} concentration (1.0 mM). More crucially, only Mg^{2+} ions residing near the core of the rRNA, where there is an overwhelming number of phosphate groups, are able to participate in inner−inner bridging (yellow and purple regions in Figure 6). Such bridging is also seen in the inner−outer and outer−outer bridging as well, albeit with a much higher probability, ∼15%. Interestingly, as the Mg^{2+} concentration decreases, the probability of finding the bridging Mg^{2+} ions in this region decreases, leading to a destabilized RNA and unfolding occurs. Our simulations, therefore, suggest that the presence of excess Mg^{2+} ions in this region, especially bridging Mg^{2+}, plays a vital role in driving the RNA to the folded structure.

DISCUSSION

Binding of Mg^{2+} and Ca^{2+} Is Nucleotide Specific. Using simulations based on the accurate TIS model, which treats divalent cations explicitly and monovalent cations implicitly, we have established that divalent cations bind with a high degree of specificity to the phosphate groups in RNA. This finding is in sharp contrast with the usual assumption that ions (often referred to as diffuse ions) are randomly localized around RNA merely to renormalize the charge on the phosphate groups. This assumption is based on the CIC theory that is strictly applicable to only rod-like or spherical polyelectrolytes (PEs),[22,23] and not to PEs with irregular shapes containing grooves. In the context of RNA folding, we find that the binding specificity depends on the nucleotide position in the folded state of the RNA. Surprisingly, the specificity of binding also depends on the nature of the intermediate states populated along the folding pathways. This implies that, even at extremely low divalent ion concentrations, interactions with RNA result in structure formation.[26] More importantly, there is a high degree of ion−ion coordination in the association of divalent cations, which again depends on the architecture of the folded states.

We also find that the majority of divalent cations binds directly to the phosphate groups in RNA using inner or outer sphere coordination. The needed screening of phosphate charges is left to monovalent ions, which are always present in the buffer or can also be increased externally. This new physical picture, based on theory and simulations, explains why only a "trace" amount of divalent ions is needed to significantly enhance RNA stability compared to monovalent ions. A rule of thumb in several experiments is that roughly 100 units of monovalent ions is needed to replace 1 unit of divalent ions.[56] For example, *Tetrahymena* ribozyme folds at around 1 M monovalent ion (perhaps not to the functionally competent state) but requires only ∼5 mM divalent cation.[4,57]

Divalent Charge Density Dictates Inner vs Outer Shell Binding. Perhaps, the most significant finding of the present study is that there are distinct chelation modes in the interaction of divalent cations with RNA during the folding process. To the best of our knowledge, the present work and a related previous study[40] are the only ones to establish that RNA stability depends on the inner and outer shell binding of divalent ions to the RNA phosphate groups. In particular, we have shown that the charge density of the ions has a strong effect on how divalent ions bind to the phosphate groups in RNA. In BWYV PK, Mg^{2+} preferentially binds to the outer shell. However, with reduced probability, some Mg^{2+} ions are also localized near the RNA core, which requires modest dehydration to bind to phosphates in the inner shell. For the larger (58-nt) fragment of the rRNA, the RNA-generated negative electrostatic potential is high enough to compensate for the high dehydration penalty of Mg^{2+}, resulting in more ions that bind to the inner shell. Indeed, in the 58-nt rRNA, the preferred mode of binding is to the inner shell. For more complex RNAs, it is likely that there would be even more Mg^{2+} ions binding directly to the phosphate groups. This accords well with the observation that most of the inner shell binding of Mg^{2+} ions is detected only for sufficiently large RNA structures.[36] For instance, the majority of Mg^{2+} ions in the crystal structure of the P4−P6 domain of the *Tetrahymena* group I intron binds in the inner shell.

For Ca^{2+}, which has a lower charge density compared to Mg^{2+}, the situation is different. In particular, Ca^{2+} ions prefer binding directly to RNA using the inner shell coordination *regardless* of the size of the RNA molecules. Dehydration of Ca^{2+} ions is readily achieved because of the lower charge density, which makes it possible to coordinate with the phosphate group through the inner shell. The dramatic shift in the binding pattern illustrated here between the two divalent ions demonstrates the exquisite dependence of the ion−RNA interaction on the cation charge density, which has also been illustrated previously using simulations and experiment.[57]

Bridging Interactions Play an Important Role in RNA Stability. Divalent ions are required to bring non-neighboring phosphate groups together to facilitate tertiary structure formation. Our simulations show that this is indeed the case, and in the process, the bridging ions play a crucial role in

https://dx.doi.org/10.1021/acs.jpcb.0c02371
J. Phys. Chem. B 2020, 124, 4114−4122

facilitating RNA folding. Once the divalent ion concentration is sufficiently low, leading to decreased probability of forming bridging ions, the tertiary structure loses stability, and the RNA eventually unfolds. Interestingly, the majority of Mg^{2+} ions engages in outer shell coordination if they bridge two non-neighboring phosphate groups. This finding is reasonable because it would be free energetically prohibitive for Mg^{2+} to dehydrate twice in order to accommodate two phosphate groups in the inner shell. The only instance this occurs in our simulations is near the core of the RNA where there is limited space and an overwhelming number of phosphate groups. Even in this extreme case, the probability of the inner−inner bridging is very small, around 2%.

Ion−DNA Interactions. Toroid formation in DNA or, in general, DNA condensation (referred to as Ψ condensation) could also be driven by Mg^{2+}.[58,59] Because the theory presented here is general, we believe that Mg^{2+} coordination to the phosphate groups in DNA is likely to occur preferentially by outer shell binding. It would be most interesting to examine the sequence-specific binding of divalent cations to DNA in order to provide a molecular basis of Mg^{2+}-induced flexibility and the mechanism of Ψ condensation.[60,61]

CONCLUSIONS

Combining an accurate treatment of the divalent ion−phosphate interactions based on RISM theory and simulations of RNA based on the transferable coarse-grained TIS force field, we have shown that the majority of divalent ions binds to RNA using either inner or outer shell coordination to phosphate groups. There is a negligible number of diffuse ions, which means binding is highly specific. This is in sharp contrast with the conventional view from counterion condensation theory, in which most of the ions are predicted to bind in a diffusive manner. Most importantly, the charge density of the cation is the driving factor in determining the ion chelation modes. Mg^{2+}, which has a small radius and therefore a high charge density, has a relatively balanced distribution between the two binding modes. On the other hand, larger ions, such as Ca^{2+}, predominantly bind using the inner sphere coordination. In addition, we also argue that, as the RNA becomes larger, there is a shift to the inner shell binding. These predictions provide an interesting new outlook of the interplay between ion−RNA interactions in the context of RNA folding. Our predictions await new experiments.

AUTHOR INFORMATION

Corresponding Author

D. Thirumalai − *Department of Chemistry, The University of Texas at Austin, Austin, Texas 78712, United States;* orcid.org/0000-0003-1801-5924; Email: dave.thirumalai@gmail.com

Author

Hung T. Nguyen − *Department of Chemistry, The University of Texas at Austin, Austin, Texas 78712, United States*

Complete contact information is available at: https://pubs.acs.org/10.1021/acs.jpcb.0c02371

Notes

The authors declare no competing financial interest.

ACKNOWLEDGMENTS

It is a pleasure to dedicate this Article to Peter Rossky whose profound contributions to our understanding of charged systems and many other topics have inspired one of us (D.T.) for decades. We are grateful to Naoto Hori for useful discussions and critical reading of the manuscript. This work was supported by NSF Grant CHE 19-00093 and the Welch Foundation Grant F-0019 through the Collie−Welch chair. We thank the Texas Advanced Computing Center for providing computational resources.

REFERENCES

(1) Tinoco, I.; Bustamante, C. How RNA Folds. *J. Mol. Biol.* **1999**, *293*, 271−281.

(2) Thirumalai, D.; Hyeon, C. RNA and Protein Folding: Common Themes and Variations. *Biochemistry* **2005**, *44*, 4957−4970.

(3) Sun, L.-Z.; Zhang, D.; Chen, S.-J. Theory and Modeling of RNA Structure and Interactions with Metal Ions and Small Molecules. *Annu. Rev. Biophys.* **2017**, *46*, 227−246.

(4) Heilman-Miller, S. L.; Thirumalai, D.; Woodson, S. A. Role of Counterion Condensation in Folding of the Tetrahymena Ribozyme. I. Equilibrium Stabilization by Cations. *J. Mol. Biol.* **2001**, *306*, 1157−1166.

(5) Pan, J.; Thirumalai, D.; Woodson, S. A. Magnesium-Dependent Folding of Self-Splicing RNA: Exploring the Link between Cooperativity, Thermodynamics, and Kinetics. *Proc. Natl. Acad. Sci. U. S. A.* **1999**, *96*, 6149−6154.

(6) Russell, R.; Millett, I. S.; Doniach, S.; Herschlag, D. Small Angle X-ray Scattering Reveals a Compact Intermediate in RNA Folding. *Nat. Struct. Biol.* **2000**, *7*, 367−370.

(7) Thirumalai, D.; Lee, N.; Woodson, S. A.; Klimov, D. Early Events in RNA Folding. *Annu. Rev. Phys. Chem.* **2001**, *52*, 751−762.

(8) Klein, D. J.; Moore, P. B.; Steitz, T. A. The Contribution of Metal Ions to the Structural Stability of the large Ribosomal Subunit. *RNA* **2004**, *10*, 1366−1379.

(9) Draper, D. E. A Guide to Ions and RNA Structure. *RNA* **2004**, *10*, 335−343.

(10) Woodson, S. A. Metal Ions and RNA Folding: a Highly Charged Topic with a Dynamic Future. *Curr. Opin. Chem. Biol.* **2005**, *9*, 104−109.

(11) Noeske, J.; Schwalbe, H.; Wohnert, J. Metal-Ion Binding and Metal-Ion Induced Folding of the Adenine-Sensing Riboswitch Aptamer Domain. *Nucleic Acids Res.* **2007**, *35*, 5262−5273.

(12) Sigel, R. K. O.; Pyle, A. M. Alternative Roles for Metal Ions in Enzyme Catalysis and the Implications for Ribozyme Chemistry. *Chem. Rev.* **2007**, *107*, 97−113.

(13) Sigel, R. K. O.; Sigel, H. A Stability Concept for Metal Ion Coordination to Single-Stranded Nucleic Acids and Affinities of Individual Sites. *Acc. Chem. Res.* **2010**, *43*, 974−984.

(14) Wong, G. C.; Pollack, L. Electrostatics of Strongly Charged Biological Polymers: Ion-Mediated Interactions and Self-Organization in Nucleic Acids and Proteins. *Annu. Rev. Phys. Chem.* **2010**, *61*, 171−189.

(15) Petrov, A. S.; Bowman, J. C.; Harvey, S. C.; Williams, L. D. Bidentate RNA-Magnesium Clamps: On the Origin of the Special Role of Magnesium in RNA Folding. *RNA* **2011**, *17*, 291−297.

(16) Hayes, R. L.; Noel, J. K.; Mohanty, U.; Whitford, P. C.; Hennelly, S. P.; Onuchic, J. N.; Sanbonmatsu, K. Y. Magnesium Fluctuations Modulate RNA Dynamics in the SAM-I Riboswitch. *J. Am. Chem. Soc.* **2012**, *134*, 12043−12053.

(17) Kirmizialtin, S.; Pabit, S.; Meisburger, S.; Pollack, L.; Elber, R. RNA and Its Ionic Cloud: Solution Scattering Experiments and Atomically Detailed Simulations. *Biophys. J.* **2012**, *102*, 819−828.

(18) Bowman, J. C.; Lenz, T. K.; Hud, N. V.; Williams, L. D. Cations in Charge: Magnesium Ions in RNA Folding and Catalysis. *Curr. Opin. Struct. Biol.* **2012**, *22*, 262−272.

(19) Lipfert, J.; Doniach, S.; Das, R.; Herschlag, D. Understanding Nucleic Acid-Ion Interactions. *Annu. Rev. Biochem.* **2014**, *83*, 813−841.
(20) Panja, S.; Hua, B.; Zegarra, D.; Ha, T.; Woodson, S. A. Metals Induce Transient Folding and Activation of the Twister Ribozyme. *Nat. Chem. Biol.* **2017**, *13*, 1109−1114.
(21) Welty, R.; Pabit, S. A.; Katz, A. M.; Calvey, G. D.; Pollack, L.; Hall, K. B. Divalent Ions Tune the Kinetics of a Bacterial GTPase Center rRNA Folding Transition from Secondary to Tertiary Structure. *RNA* **2018**, *24*, 1828−1838.
(22) Oosawa, F. *Polyelectrolytes*, 1st ed.; M. Dekker: New York, 1971.
(23) Manning, G. S. The Molecular Theory of Polyelectrolyte Solutions with Applications to the Electrostatic Properties of Polynucleotides. *Q. Rev. Biophys.* **1978**, *11*, 179−246.
(24) Heilman-Miller, S. L.; Pan, J.; Thirumalai, D.; Woodson, S. A. Role of Counterion Condensation in Folding of the Tetrahymena Ribozyme II. Counterion-dependence of Folding Kinetics. *J. Mol. Biol.* **2001**, *309*, 57−68.
(25) Hori, N.; Denesyuk, N. A.; Thirumalai, D. Ion Condensation onto Ribozyme is Site Specific and Fold Dependent. *Biophys. J.* **2019**, *116*, 2400−2410.
(26) Denesyuk, N. A.; Thirumalai, D. How do Metal Ions Direct Ribozyme Folding? *Nat. Chem.* **2015**, *7*, 793−801.
(27) Giambasu, G. M.; Case, D. A.; York, D. M. Predicting Site-Binding Modes of Ions and Water to Nucleic Acids Using Molecular Solvation Theory. *J. Am. Chem. Soc.* **2019**, *141*, 2435−2445.
(28) Krasovska, M. V.; Sefcikova, J.; Reblova, K.; Schneider, B.; Walter, N. G.; Sponer, J. Cations and Hydration in Catalytic RNA: Molecular Dynamics of the Hepatitis Delta Virus Ribozyme. *Biophys. J.* **2006**, *91*, 626−638.
(29) Do, T. N.; Ippoliti, E.; Carloni, P.; Varani, G.; Parrinello, M. Counterion Redistribution upon Binding of a Tat-Protein Mimic to HIV-1 TAR RNA. *J. Chem. Theory Comput.* **2012**, *8*, 688−694.
(30) Bergonzo, C.; Hall, K. B.; Cheatham, T. E. Stem-Loop V of Varkud Satellite RNA Exhibits Characteristics of the Mg^{2+} Bound Structure in the Presence of Monovalent Ions. *J. Phys. Chem. B* **2015**, *119*, 12355−12364.
(31) Lemkul, J. A.; Lakkaraju, S. K.; MacKerell, A. D. Characterization of Mg^{2+} Distributions around RNA in Solution. *ACS Omega* **2016**, *1*, 680−688.
(32) Lee, T.-S.; Radak, B. K.; Harris, M. E.; York, D. M. A Two-Metal-Ion-Mediated Conformational Switching Pathway for HDV Ribozyme Activation. *ACS Catal.* **2016**, *6*, 1853−1869.
(33) Sun, L.-Z.; Chen, S.-J. Predicting RNA-Metal Ion Binding with Ion Dehydration Effects. *Biophys. J.* **2019**, *116*, 184−195.
(34) Kostenbader, K.; York, D. M. Molecular Simulations of the Pistol Ribozyme: Unifying the Interpretation of Experimental Data and Establishing Functional Links with the Hammerhead Ribozyme. *RNA* **2019**, *25*, 1439−1456.
(35) Ganguly, A.; Weissman, B. P.; Giese, T. J.; Li, N.-S.; Hoshika, S.; Rao, S.; Benner, S. A.; Piccirilli, J. A.; York, D. M. Confluence of Theory and Experiment Reveals the Catalytic Mechanism of the Varkud Satellite Ribozyme. *Nat. Chem.* **2020**, *12*, 193−201.
(36) Cate, J. H.; Hanna, R. L.; Doudna, J. A. A Magnesium Ion Core at the Heart of a Ribozyme Domain. *Nat. Struct. Biol.* **1997**, *4*, 553−558.
(37) Pettitt, B. M.; Rossky, P. J. Integral Equation Predictions of Liquid State Structure for Waterlike Intermolecular Potentials. *J. Chem. Phys.* **1982**, *77*, 1451−1457.
(38) Hirata, F.; Rossky, P. J.; Pettitt, B. M. The Interionic Potential of Mean Force in a Molecular Polar Solvent from an Extended RISM Equation. *J. Chem. Phys.* **1983**, *78*, 4133−4144.
(39) Pettitt, B. M.; Rossky, P. J. Alkali Halides in Water: Ion-Solvent Correlations and Ion-Ion Potentials of Mean Force at Infinite Dilution. *J. Chem. Phys.* **1986**, *84*, 5836−5844.
(40) Nguyen, H. T.; Hori, N.; Thirumalai, D. Theory and Simulations for RNA Folding in Mixtures of Monovalent and Divalent Cations. *Proc. Natl. Acad. Sci. U. S. A.* **2019**, *116*, 21022−21030.
(41) Hyeon, C.; Thirumalai, D. Mechanical Unfolding of RNA Hairpins. *Proc. Natl. Acad. Sci. U. S. A.* **2005**, *102*, 6789−6794.
(42) Chandler, D.; Andersen, H. C. Optimized Cluster Expansions for Classical Fluids. II. Theory of Molecular Liquids. *J. Chem. Phys.* **1972**, *57*, 1930−1937.
(43) Luchko, T.; Joung, I. S.; Case, D. A. *Innovations in Biomolecular Modeling and Simulations: Vol. 1*; The Royal Society of Chemistry: London, 2012; Vol. *1*, pp 51−86.
(44) Rodgers, J. M.; Weeks, J. D. Local Molecular Field Theory for the Treatment of Electrostatics. *J. Phys.: Condens. Matter* **2008**, *20*, 494206.
(45) Remsing, R. C.; Liu, S.; Weeks, J. D. Long-Ranged Contributions to Solvation Free Energies from Theory and Short-Ranged Models. *Proc. Natl. Acad. Sci. U. S. A.* **2016**, *113*, 2819−2826.
(46) Gao, A.; Remsing, R. C.; Weeks, J. D. Short Solvent Model for Ion Correlations and Hydrophobic Association. *Proc. Natl. Acad. Sci. U. S. A.* **2020**, *117*, 1293−1302.
(47) Denesyuk, N. A.; Thirumalai, D. Coarse-Grained Model for Predicting RNA Folding Thermodynamics. *J. Phys. Chem. B* **2013**, *117*, 4901−4911.
(48) Honeycutt, J. D.; Thirumalai, D. The Nature of Folded States of Globular Proteins. *Biopolymers* **1992**, *32*, 695−709.
(49) Grilley, D.; Misra, V.; Caliskan, G.; Draper, D. E. Importance of Partially Unfolded Conformations for Mg^{2+}-Induced Folding of RNA Tertiary Structure: Structural Models and Free Energies of Mg^{2+} Interactions. *Biochemistry* **2007**, *46*, 10266−10278.
(50) Lee, Y.; Thirumalai, D.; Hyeon, C. Ultrasensitivity of Water Exchange Kinetics to the Size of Metal Ion. *J. Am. Chem. Soc.* **2017**, *139*, 12334−12337.
(51) Zheng, H.; Shabalin, I. G.; Handing, K. B.; Bujnicki, J. M.; Minor, W. Magnesium-Binding Architectures in RNA Crystal Structures: Validation, Binding Preferences, Classification and Motif Detection. *Nucleic Acids Res.* **2015**, *43*, 3789−3801.
(52) Leonarski, F.; D'Ascenzo, L.; Auffinger, P. Mg^{2+} Ions: Do They Bind to Nucleobase Nitrogens? *Nucleic Acids Res.* **2017**, *45*, 987−1004.
(53) Egli, M.; Minasov, G.; Su, L.; Rich, A. Metal Ions and Flexibility in a Viral RNA Pseudoknot at Atomic Resolution. *Proc. Natl. Acad. Sci. U. S. A.* **2002**, *99*, 4302−4307.
(54) Andresen, K.; Das, R.; Park, H. Y.; Smith, H.; Kwok, L. W.; Lamb, J. S.; Kirkland, E. J.; Herschlag, D.; Finkelstein, K. D.; Pollack, L. Spatial Distribution of Competing Ions around DNA in Solution. *Phys. Rev. Lett.* **2004**, *93*, 248103.
(55) Nguyen, H. T.; Pabit, S. A.; Pollack, L.; Case, D. A. Extracting Water and Ion Distributions from Solution X-ray Scattering Experiments. *J. Chem. Phys.* **2016**, *144*, 214105.
(56) Owczarzy, R.; Moreira, B. G.; You, Y.; Behlke, M. A.; Walder, J. A. Predicting Stability of DNA Duplexes in Solutions Containing Magnesium and Monovalent Cations. *Biochemistry* **2008**, *47*, 5336−5353.
(57) Koculi, E.; Hyeon, C.; Thirumalai, D.; Woodson, S. A. Charge Density of Divalent Metal Cations Determines RNA Stability. *J. Am. Chem. Soc.* **2007**, *129*, 2676−2682.
(58) Rau, D. C.; Parsegian, V. A. Direct Measurement of the Intermolecular Forces between Counterion-Condensed DNA Double Helices. *Biophys. J.* **1992**, *61*, 246−259.
(59) Bloomfield, V. A. DNA Condensation by Multivalent Cations. *Biopolymers* **1997**, *44*, 269−282.
(60) Baumann, C. G.; Smith, S. B.; Bloomfield, V. A.; Bustamante, C. Ionic Effects on the Elasticity of Single DNA Molecules. *Proc. Natl. Acad. Sci. U. S. A.* **1997**, *94*, 6185−6190.
(61) Lee, N.; Thirumalai, D. Stretching DNA: Role of Electrostatic Interactions. *Eur. Phys. J. B* **1999**, *12*, 599−605.

https://dx.doi.org/10.1021/acs.jpcb.0c02371
J. Phys. Chem. B 2020, 124, 4114−4122